SLAC-PUB-3628
CALT-68-1262
April 1985
(T/E)

Measurement of D^0 Lifetime in e^+e^- Annihilation at High Energy*

H.Yamamoto, W.B.Atwood, P.H.Baillon[a], B.C.Barish, G.R.Bonneaud, A.Courau, G.J.Donaldson[b], R.Dubois[c], M.M.Duro, E.E.Elsen[d], S.G.Gao[e], Y.Z.Huang[f], G.M.Irwin, R.Johnson, H.Kichimi[g], J.Kirkby[a], D.E.Klem, D.E.Koop[h], J.Ludwig[i], G.B.Mills, A.Ogawa, T.Pal, D.Perret-Gallix[j], R.Pitthan, D.L.Pollard[k], C.Y.Prescott, L.Z.Rivkin, L.S.Rochester, W.Ruckstuhl[l], M.Sakuda, S.Sherman[m], E.J.Siskind[n], R.Stroynowski, S.Q.Wang,[f] S.G.Wojcicki, W.G.Yan,[f] C.C.Young,

DELCO Collaboration

California Institute of Technology,

Pasadena, California 91125

Stanford Linear Accelerator Center and Physics Department

Stanford University, Stanford, California 94305

Submitted to *Physical Review D*

* This work was supported in part by the Department of Energy, contract numbers DE-AC03-76SF00515 and DE-AC03-81-ER40050, and the National Science Foundation.

ABSTRACT

A measurement of D^0 lifetime using the impact parameter method is presented. The D^0 sample is obtained from identified $D^{*\pm}$ decays in e^+e^- annihilations into hadrons at a center of mass energy of 29 GeV. The maximum likelihood method used includes the effects of various backgrounds, giving the D^0 lifetime of $4.6^{+1.5}_{-1.5}(stat)^{+0.7}_{-0.6}(sys) \times 10^{-13}$ sec. The meathod is found to be consistent and bias free. Together with the semileptonic branching ratio of D^0, the effective charm quark mass is obtained.

1. Introduction

Charmed mesons continue to provide us with many puzzles as well as clues to the structure and decay mechanism of hadrons. Among the most intriguing is the difference in the lifetime and semileptonic branching fraction of D^0 and $D^{\pm}$ mesons.[1,2] If the charm quark decays independently of the light quark (spectator model) then the lifetime and the semileptonic branching fraction should be identical for both mesons. Two types of attempts have been made to accommodate the difference in the framework of the standard model. One is to explain an enhancement of the non-leptonic decay rate of D^0 and the other is to account for a suppression of the $D^{\pm}$ non-leptonic decays.[3] In both approaches, the light quark typically plays an important role (non-spectator models) in the non-leptonic decays while the semileptonic decay rate is assumed to be the same for both mesons at least up to the Cabbibo suppression.[4–6] Measuring the lifetimes and/or the semileptonic branching fractions of both mesons provides important information on which of the two is more important. Moreover, the lifetime and the semileptonic branching ratio together give an absolute measurement of the semileptonic decay rate which can be compared with theoretical predictions. Thus, the measurements of the lifetimes and the semileptonic branching ratios are complementary to each other, and together they can put strong constraints on our understanding of heavy meson decays.

The lifetime of D^0 has been measured in various environments[7] including e^+e^- annihilations[8] where the crossing point of the two tracks from each D^0 decay is measured with respect to the center of the beam. In this report is described a measurement of the D^0 lifetime in the e^+e^- interactions by a method using the impact parameter of the D^0 decay tracks, which is found to be insensitive to a

wide range of background effects.

2. Procedure

The D^0 candidates are selected in the decays of charged D^*'s

$$D^{*+} \to D^0 \pi^+_{D^*}, \quad \text{and} \quad D^0 \to K^- \pi^+ (X), \tag{2.1}$$

(and its charge conjugate) where X, which is not observed, is typically a π^0, and the subscript 'D^*' of the first pion is to distinguish it from the pion in the D^0 decay. For each of the two charged tracks from the D^0 decay, the impact parameter b is defined in the plane perpendicular to the beam axis (xy plane) and with respect to the beam center measured by the beam position monitor (Fig. 1). The sign is defined to be positive if the inner product of the D^0 momentum in xy plane, $\vec{P}_{\perp D^0}$, and the vector from the beam center to the point of closest approach on the track, $\vec{b}$, is positive, and negative if the inner product is negative. The two cases are shown in Fig. 1.

If a D^0 is created at the beam center given by the monitor, and if the D^0 decay track is measured without errors, then the impact parameter b is always positive and given by $d_\perp \sin\theta$, where $d_\perp$ is the D^0 decay distance projected onto the xy plane, and θ is the angle between $P_{\perp D^0}$ and the track direction in the xy plane.

The true impact parameter distribution is smeared by measurement errors and because the true primary vertex is only approximated by the beam center given by the monitor. As shown in detail in later sections, these errors can be well approximated by a gaussian plus a small flat background, where the width

of the gaussian depends on the configuration of each event. The probability that a track is not from a D^0 decay also varies from event to event.

In order to extract the D^0 lifetime from the impact parameter data, we have chosen to employ a maximum likelihood method which allows us to make the most out of the information available. In the following sections we will discuss the details of the analysis.

3. Components Of Analysis

3.1 DETECTOR

The data have been collected by the DELCO detector at the PEP storage ring with a center-of-mass energy of 29 GeV. The side view of the detector is shown in Fig. 2. One of the unique features of the detector is the good particle identification capability provided by its gas threshold Čerenkov counter.[9] The Čerenkov counter consists of 36 cells which cover 62% of 4π. Only the data taken with isobutane gas is used for this analysis, with an integrated luminosity of 150 pb^{-1}. Each cell is viewed by a RCA 8854 quantacon phototube coated with paraterphenyl to enhance the light collection in UV region, which collects an average of 18 photoelectrons for a Bhabha track. The threshold momentum is 2.6 and 9.2 GeV/c for pions and kaons respectively.

The Čerenkov counter is sandwiched by inner and outer drift chambers. The inner chambers consist of 6 layers (uuzzvv) of Inner Drift Chamber, or IDC, and 10 layers (zzuuzzvvzz) of Central Drift Chamber, or CDC, where, in the parentheses, z indicates a layer with wires parallel to the beam axis, and u and v are layers with small angle stereo wires (about ± 2 degrees). The innermost

layer of the IDC is at $r = 12.0$ cm and the outer most layer of the CDC is at 48.9 cm. The single hit position resolution for a Bhabha track is 140 μm for the IDC and 200 μm for the CDC. It leads to the impact parameter resolution of 230 μm without fixing the momentum of Bhabha tracks to the beam energy and without track origin constraint. The outer drift chambers are made of 6 modules of planar chambers that form a hexagon. Each module contains 6 layers (zzuvzz), where u and v are large angle ($\pm$30 degrees) stereo layers. The single hit resolution of the outer chambers is 450 μm. The magnet is of the Helmholtz type in order to reduce the amount of material before the Čerenkov counter. The field is 3.3 kG at the center and the total $\int Bdl$ is 1.8 kG·m. The resulting momentum resolution is $\sigma_P/P = \sqrt{(2\%P)^2 + (6\%)^2}$ where P is in GeV/c.

3.2 Beam Position Monitor

The beam position monitors are located $\pm$3.74m from the interaction point. Each consists of four electrodes (buttons) placed inside the vacuum pipe which pick up pulses induced by the passing beam bunches. A total of eight pulse heights from the buttons are recorded for the bunch corresponding to each event and from these the beam centroid position at the interaction region is calculated event by event.

In Fig. 3, the interaction points of Bhabha events are compared with the beam center measured by the monitor. For a Bhabha track that is emitted almost vertically (within $\pm$0.25 radian in ϕ), the x coordinate of the vertex is well approximated by the x coordinate of the origin of the track. The y coordinate is obtained similarly using the tracks emitted almost horizontally (within $\pm$0.20 radian). Fig. 3(a) and (b) show the x coordinate values in the laboratory frame

and relative to the beam position monitor value, respectively. Fig. 3(c) and (d) show the same for the y coordinate. Even though the fluctuation of the beam position is as large as 3 mm, it can be seen that the beam position monitor is tracking the true beam center reasonably well.

3.3 Beam Sizes

There are three data blocks with somewhat different configurations which correspond to the three operational years, 1982, '83, and '84. The tracking qualities are roughly the same for the three, even though the '83 data have slightly worse position resolutions than the rest.

The beam cross section can be approximated by a 2-dimensional gaussian with widths σ_x and σ_y. Then the error in the impact parameter due to the beam size at an azimuthal angle ϕ is given by,

$$\sigma_{\rm beam}(\phi)^2 = \sigma_x^2 \cos^2\phi + \sigma_y^2 \sin^2\phi. \tag{3.1}$$

The beam size is obtained by measuring the width of the impact parameter distribution of Bhabha tracks and then subtracting the measurement error in quadrature, where the measurement error is estimated by the track separation distance near the beam. Fig. 4 shows the measured $\sigma^2_{\rm beam}$ as a function of ϕ for the '83 data. The smooth curve is a fit to the expected shape (3.1) with σ_x and σ_y as parameters. The results are summarized in Table 1 for the three datasets. The values expected from the machine parameters of the storage ring[10] are also listed. The espected values are naive theoretical predictions and can include systematic errors such as the beam-beam interactions. Also, it is worth noting that the

measured beam sizes are the true beam sizes convoluted with the resolution of the beam position monitor, which are exactly what we need for the fit of D^0 lifetime since the D^0 tracks are also measured with respect to the beam position given by the monitor.

3.4 Measurement Error In Hadronic Events

There are three contributions to the impact parameter error σ

$$\sigma^2 = \sigma^2_{\text{beam}} + \sigma^2_{\text{m.s.}} + \sigma^2_{\text{trk}}, \tag{3.2}$$

where

σ_{beam} is given by (3.1),

$\sigma_{\text{m.s.}}$ is due to multiple scattering at the beam pipe and the inner wall of IDC, and

σ_{trk} is due to tracking errors inside the drift chambers.

We use the following formula[11] for $\sigma_{\text{m.s.}}$

$$\sigma_{\text{m.s.}} = \frac{r_{\text{eff}}}{\cos\lambda}\frac{0.0141}{P\beta}\sqrt{\frac{X}{\cos\lambda}}\left(1+\frac{1}{9}\log_{10}\frac{X}{\cos\lambda}\right), \tag{3.3}$$

where

r_{eff} is the effective average radius of the materials before the tracking volume, which is 9.1 cm and 9.0 cm for the '82/3 datasets and the '84 dataset respectively.

λ is the angle of the track away from the plane perpendicular to the beam axis,

P, β are the momentum (in GeV/c) and the velocity of the particle, and

X is the total amount of material in the direction perpendicular to the beam axis (in radiation length), which is 2.25% and 1.28% for the '82/3 datasets and the '84 dataset respectively.

This formula is good to a few percent in the cases of interest. There are, however, non-gaussian components due to plural and single scatterings. They will be treated as part of a flat background.

The error $\sigma_{\rm trk}$ includes the measurement error of each drift chamber hit, the effect of taking wrong hits (i.e. the partial confusion in tracking), and the effect of multiple scattering inside the tracking volume due to the gas, wires, and other materials along a track.

The track fitting program returns an estimated error for the impact parameter, $\sigma_{\rm fit}$, assuming that all the points associated with the track are correct and the measurement error of each point is properly estimated. Even though it is a useful indication of the quality of the measured impact parameter, a correction has to be made to obtain a realistic $\sigma_{\rm trk}$ in actual hadronic events.

In order to obtain the functional form of the correction, general hadronic tracks are divided into $\sigma_{\rm fit}$ bins. In each bin the impact parameter distribution is fitted with a gaussian plus a flat background that is expected from strange particle decays and nuclear interactions etc.[12] Also, the root-mean-squares of $\sigma_{\rm m.s.}$ and $\sigma_{\rm beam}$ are calculated for the tracks in each $\sigma_{\rm fit}$ bin and are quadratically subtracted from the measured width to get $\sigma_{\rm trk}$. Fig. 5 shows the resulting $\sigma_{\rm trk}$ as a function of $\sigma_{\rm fit}$. The broken lines show the root-mean-squares of $\sigma_{\rm m.s.}$ and $\sigma_{\rm beam}$ which have been subtracted in each bin. The curve is a fit to the correction function.

We can now estimate the overall error in the impact parameter by the formula

(3.2). In Fig. 6, the impact parameter distribution is shown for each σ bin. The curve in each plot is the result of fit with a gaussian plus a flat background, where the width of gaussian is fixed to the expected value.

3.5 D^0 Track Selection

The D^0 tracks are selected as the decay products of charged D^*'s in the decay chain (2.1). The method takes advantage of the low Q value of the D^* decay that limits the phase space thus suppressing the random background.[13] In this analysis, we further enhance the signal by using the Čerenkov counter to select the kaon or the pion from the D^0 decay.[14] Kaon candidates are selected by requiring tracks with P greater than 3.2 GeV/c to have no response in the associated Čerenkov cell. On the other hand, the criteria for pion candidates are: $2.6 < P < 9$ GeV/c, and that the associated Čerenkov cell has a response of more than 3 photoelectrons. These kaon and pion candidate tracks have substantial momenta, and are called 'leading' tracks. Each of them is then combined with another track of the opposite sign (non-leading track) to form a D^0 candidate. When the leading track is a kaon (pion) candidate, we call it a K-mode (π-mode) combination. For a K-mode candidate, the kaon mass is assigned to the leading track and the pion mass is assigned to the non-leading track. For a π-mode candidate, the mass assignments are inverted accordingly. After the invariant mass cut of $1.45 < M_{K\pi} < 2.2$ GeV/c^2, each D^0 candidate is combined with another track (π_{D^*} candidate) within the cone of $\sin\theta_{D^0\pi_{D^*}} < 0.13$. The π_{D^*} candidate track is said to be 'wrong' sign if its charge is the same as that of the track assigned the kaon mass, and 'right' sign if not. The mass difference $\Delta M = M_{K\pi\pi_{D^*}} - M_{K\pi}$ is plotted in Fig. 7 for both the K-mode and π-mode

samples. The enhancement of the right sign is clear for both cases. The signal region is taken to be $\Delta M < 0.1625$ GeV/c^2.

Without any further cuts, there are 104 K-mode D^* candidates and 122 π-mode D^* candidates in the right sign sample. There are 18 candidates overlapping the two modes which we have classified as K-modes.

Then the following cuts are made to the D^0 tracks:

1. P greater than 250 MeV/c. This is to reject tracks with a very large error in impact parameter: it rejects 5 out of the 452 tracks.
2. $\eta \sin\theta > 0.4$, where $\eta \equiv P_{\perp D^0}/M_{D^0}$ and θ is defined in Fig. 1. This is the ratio of the impact parameter to the decay distance of D^0 when errors are ignored. The larger this value is, the more weight the track has in the lifetime determination. And if it is zero, the track does not contribute to the lifetime measurement. Thus, even though this cut eliminates 173 out of 447 tracks, it does not degrade the statistical error of the fit while making it less sensitive to the background. Fig. 8 shows the $\eta \sin\theta$ distributions for all the D^0 candidate tracks in the data. It can be seen that most of the tracks rejected are leading tracks.
3. $|b|$ <2.5 mm. This defines the window of impact parameter; it removes 5 more tracks, leaving 269.

Fig. 9 shows the impact parameter distribution after the cuts. The distribution is clearly shifted in the positive direction, and the mean of the distribution is 151.7±42.3 μm. The curve overplotted is the result of the fit described in detail later.

Three different control samples are checked:

(a) General hadronic tracks with $P > 250$ MeV/c and $|b| < 2.5$ mm, where the thrust axis is used as the D^0 direction.

(b) The sample of tracks kinematically similar to the D^0 tracks. It is formed by taking all the D^0 candidates selected just as before but without the information of the Čerenkov counter and without combining them with π_{D^*} candidates.

(c) The same as (a), except that for each event the thrust axis of the previous event is used as the D^0 direction.

The impact parameter distributions for the three cases are shown in Fig. 10, and the results are summarized in Table 2. The expected values from the Monte Carlo[15] are also included in the table. Positive means for the case (a) and (b) are expected because of strange and heavy particle decays.

The mean of the impact parameter is not shifted by nuclear interactions and Coulomb scattering at the beam pipe region or by small misalignments of the drift chambers etc. The changes in the measured impact parameter due to these sources are expected to be symmetric and do not alter the mean value, while they increase the width slightly. This point is demonstrated by the control sample (c) in which the thrust axis is randomized. The mean becomes consistent with zero for both the data and the Monte Carlo.

3.6 Estimation Of Background

Non-D^0 tracks To study non-D^0 background, we compare the right and wrong sign samples. The background in the D^* sample is expected to have the same amount of right and wrong sign combinations. Therefore, the number of right signs minus the number of wrong signs indicates the number of true D^*'s for

which both the leading track and the π_{D^*} track are found correctly. However, the non-leading tracks populate the same momentum region as the average hadronic tracks and are more easily contaminated than the leading tracks. Also, the Cabibbo-suppressed decays of D^0 that generate a wrong sign kaon can contribute to the wrong sign K-mode sample. In addition, when a D^0 decay contains multiple charged pions, a wrong sign pion can become the leading pion candidate thus contributing to the wrong sign π-mode sample even if the tracks are genuinely from a D^*. Therefore, the number of right signs minus wrong signs has to be multiplied by a correction factor to get the number of candidates for which the track of interest is correctly found. We assume the $D^0 - \bar{D}^0$ mixing to be negligible.[14]

The correction factor $r_{\rm corr}$ is given by the Monte Carlo according to

$$r_{\rm corr} = \frac{(\#\text{ of correct tracks in the right sign sample})}{(\#\text{ of right signs}) - (\#\text{ of wrong signs})}.$$

Table 3 summarizes the result. The first errors in the purities (probabilities that a track is from a D^0 decay) are statistical and the second errors are systematic. The systematic errors are due to the uncertainty in the correction factors. For the leading tracks, the uncertainty comes mostly from our imperfect knowledge of the D^0 decay branching fractions and their kinematics, and the non-leading tracks have a further systematic error corresponding to the added contamination.

<u>D^*'s from b-quarks</u> Since the decay of a b-quark almost always creates a c-quark,[16] we expect some of the D^*'s in our dataset to come from decays of b-flavored particles. The average $c\tau$ of the b-hadrons is relatively long and of the order of several hundred microns,[17,18] which substantially changes the impact parameters of the D^0 tracks originating from b-flavored hadrons.

The number of D^0 tracks coming from b-quarks is estimated by the Monte Carlo using the same set of D^* selection and track cuts as for the data, where the direct production ratio of D^* to D is set to 1 in the decays of b-hadrons. The result is shown in Fig. 11 as a function of D^0 momentum P_{D^0}. The amount of contamination is similar for K tracks and π tracks and the mean of the impact parameter for these tracks, κ_b, is found to be flat in $\eta \sin\theta$. With the average b lifetime of 350 μm,[18] and the D^0 lifetime of 136 μm, κ_b is estimated to be 210 μm. It does not depend strongly on the D^0 lifetime.

4. Likelihood Fit Of D^0 Lifetime

4.1 D^0 LIFETIME LIKELIHOOD FUNCTION

For a given event configuration characterized by a set of parameters $\mathbf{a} = (a_1 ... a_m)$ and for a given D^0 lifetime τ, the distribution of measured impact parameter b, $f^0(b, l, \mathbf{a})db$, will be a function of these parameters, where $l \equiv c\tau$ and the area is normalized to unity. The superscript 0 indicates that the function is normalized in the range $(-\infty, \infty)$ of b. Typical examples of $\mathbf{a}$ are D^0 momentum, track momentum, the angle between them, track quality, and so on.

When this is viewed as a function of l, it is the likelihood function, $L(l)$, for a single event with a measured impact parameter b and an event configuration characterized by $\mathbf{a}$. It has the following procedural interpretation: If we generate l uniformly from 0 to infinity (or some large enough value) and generate many impact parameters according to the distribution given by f^0, and then select a sample of events with the impact parameters in a range $(b, b + db)$, the l's associated with these events have a distribution given by the likelihood function $L(l)$, and its maximum gives the most likely value of l.

When the range of measurable b is limited to (b_1, b_2), or equivalently when there is a window for b to be accepted, then the likelihood functions have to be normalized in the window

$$f(b^i, l, \mathbf{a}^i) \equiv \frac{f^0(b^i, l, \mathbf{a}^i)}{\int_{b_1}^{b_2} f^0(b, l, \mathbf{a}^i) db}. \tag{4.1}$$

This follows from the 'requirement of consistency', namely, the estimator should reproduce the true value when the statistics become large.[19]

For N measurements of impact parameter, b^i $(i = 1, N)$, in which each event is characterized by $\mathbf{a}^i$, the same procedural argument leads to a likelihood function,

$$L(l)dl = \left[\prod_{i=1}^{N} f(b^i, l, \mathbf{a}^i)\right] dl. \tag{4.2}$$

We can define a function $\mathcal{L}$ by

$$\mathcal{L}(l) \equiv -2 \log L(l) = -2 \sum_{i=1}^{N} \log f(b^i, l, \mathbf{a}^i) \tag{4.3}$$

If the f's are all gaussian, this is equivalent to the χ^2 up to a constant. And the one-sigma contour is defined by the points where $\mathcal{L}$ increases one unit above the minimum value. However, $\mathcal{L}$ cannot be interpreted as the χ^2 that indicates the goodness of the fit, which will be discussed later.

First we construct a single event likelihood function ignoring backgrounds. Then the likelihood function f^0 is a convolution of an exponential and a gaussian;

$$\frac{1}{\kappa} \exp\left(-\frac{b}{\kappa}\right), \qquad \frac{1}{\sqrt{2\pi}\sigma} \exp\left(-\frac{b^2}{2\sigma^2}\right),$$

where $\kappa = l\eta \sin\theta$ and σ is given by the formula (3.2). The result can be expressed

using the complementary error function,[20]

$$f^0(b,l,\mathrm{a}) \equiv f^0(b,\kappa,\sigma) = \frac{1}{2\kappa}\exp\left(\frac{\sigma^2}{2\kappa^2} - \frac{b}{\kappa}\right)\,\mathrm{erfc}\left[\frac{1}{\sqrt{2}}\left(\frac{\sigma}{\kappa} - \frac{b}{\sigma}\right)\right], \qquad (4.4)$$

where f^0 is a function of l only through κ, and both κ and σ are functions of a. The shape of f^0 as a function of b is shown in Fig. 12 for $\sigma = 500$ μm and several different κ's.

In order to take into account the effect of the impact parameter window, this formula has to be integrated from b_1 to b_2, where $b_1 = -2.5$ mm and $b_2 = 2.5$ mm. The above formula can be simplified by changing the variable,

$$f^0(b,\kappa,\sigma)db = \alpha e^{2\alpha x - \alpha^2}\mathrm{erfc}(x)\,dx$$

where

$$\alpha = \frac{\sigma}{\sqrt{2}\kappa}, \quad \text{and} \quad x = \frac{1}{\sqrt{2}}\left(\frac{\sigma}{\kappa} - \frac{b}{\sigma}\right) \qquad (4.5)$$

This can be readily integrated by interchanging the order of integrations to give

$$\int_{b_1}^{b_2} f^0(b,\kappa,\sigma)db = \frac{1}{2}\left[e^{2\alpha x - \alpha^2}\mathrm{erfc}(x) + \mathrm{erf}(x-\alpha)\right]_{x_1}^{x_2} \qquad (4.6)$$

where x_i is given by (4.5) from b_i.

The non-D^0 background is handled by adding a term which represents the distribution of the general background shape. We take it to be $\beta f^0(b,\kappa_B,\sigma)$, where β is the background fraction (1−purity) (see Table 3), σ is the expected impact parameter resolution for the track, and κ_B is a global constant that takes care of the fact that the background does include genuinely positive impact

parameters. We use a value $\kappa_B = 54.6\ \mu$m from Fig. 10(b). Even though the true distribution is not exactly a convolution of an exponential and a gaussian, this is a good enough approximation and the result is insensitive to the exact shape. The b-quark contamination is handled in the same way by adding $\delta f^0(b, \kappa_b, \sigma)$ to the likelihood function, where δ is the fraction of the tracks originating from b-quarks and κ_b is the mean impact parameter for those tracks.

The flat background of the impact parameter distribution cannot be reliably estimated *a priori* for the D^0 tracks from the general hadronic tracks because the sources of flat background are different for the two samples. Instead, we take the level of flat background γ to be the second parameter of the fit.

Putting everything together, our final properly normalized single event likelihood function is

$$f(b, l, \mathbf{a}) = A\left[(1-\beta-\delta)f^0(b,\kappa,\sigma) + \beta f^0(b,\kappa_B,\sigma) + \delta f^0(b,\kappa_b,\sigma) + \gamma\right] \quad (4.7)$$

with

$$A = \left[(1-\beta-\delta)\int_{b_1}^{b_2} f^0(b,\kappa,\sigma)db + \beta\int_{b_1}^{b_2} f^0(b,\kappa_B,\sigma)db + \delta\int_{b_1}^{b_2} f^0(b,\kappa_b,\sigma)db + (b_2-b_1)\gamma\right]^{-1}$$

where,

f^0 is a function given by the formula (4.4) and its integration is given by the formula (4.6),

$\kappa = l\eta\sin\theta$, with $\eta = P_{\perp D^0}/M_{D^0}$,

σ is the overall error in the impact parameter, and given by (3.2).

β is the background fraction and given by Table 3,

κ_B is a constant(54.6 μm) to represent the positive mean impact parameter of the background,

δ is the fraction of tracks that come from b-quarks and given by Fig. 11,

κ_b is the mean impact parameter of the D^0 tracks originating from hadrons containing b-quarks (240 μm),

γ is a constant that represents the flat background which is another parameter in the likelihood fit.

The one-sigma contour of the fit is shown in Fig. 13, and the results for the individual parameters are; $c\tau = 136 \pm 46$ μm and $\gamma = 0.078^{+0.058}_{-0.042}$ cm^{-1}. The value of γ corresponds to a flat background of about 4% of the total area. The effect of the flat background is not large.

4.2 Goodness Of Fit And Bias Check

One way to check the goodness of fit is to bin the impact parameters into a histogram and compare it to the expected shape from the result of the fit. The expected shape is given by

$$\left[\sum_{i=1}^{N} f(b, l^0, \mathbf{a}^i)\right] \Delta b,$$

where f is given by the formula (4.7), Δb is the bin width of the histogram, and the lifetime l^0 is the result of the fit. The curve is overplotted in the Fig. 9. The χ^2 of the fit is 8.9 for 10 degrees of freedom.[21]

Another way to check the fit, which is independent of the binning, makes use of the similarity between $\mathcal{L}$ and χ^2. As mentioned earlier, $\mathcal{L}$ is equivalent to χ^2 up to a constant offset when the function f's are all gaussian with each impact parameter measurement representing a single data point of the χ^2 estimation. In the case of χ^2, the expected distribution of the minimum is a function of the number of degree of freedom and is well known. For $\mathcal{L}_{\rm min}$, the expected distribution is not known *a priori*, but can be estimated by a simulation as follows. Using the result of the fit l^0, one impact parameter is generated for each track of the data according to the formula (4.7) using the same σ, κ's etc. as used in the likelihood fit. Then, taking these impact parameters as input data, the likelihood analysis is repeated and $\mathcal{L}_{\rm min}$ is calculated. The process is repeated from the beginning many times to generate the distribution of $\mathcal{L}_{\rm min}$. If the fit is good, then the measured $\mathcal{L}_{\rm min}$ should be inside the central distribution. The result is shown in Fig. 14(a). The arrow indicates the observed value of $\mathcal{L}_{\rm min}$. The goodness of the fit is reasonable with a 20% chance of getting a better $\mathcal{L}_{\rm min}$ than the one observed.

As a byproduct, the bias of the fit is checked by the distribution of $c\tau$ that corresponds to each of the $\mathcal{L}_{\rm min}$ above. It is shown in Fig. 14(b). The mean of the reconstructed $c\tau$'s agrees well with the input, namely the method is bias free within the statistical error. Also, the width of the distribution (44 μm) is in good agreement with the range of one sigma estimated by $\mathcal{L} - \mathcal{L}_{\rm min} < 1$, which is ± 46 μm.

4.3 SYSTEMATIC ERRORS

1) Non D^0 Background (β, κ_B)

The systematic errors of the estimation of non-D^0 background in Table 3 are likely to have positive correlations, and have been added linearly. The statistical errors in Table 3, on the other hand, are added quadratically. The combined error in $c\tau$ is found to be symmetric and ± 4 μm. The other parameter related to the non-D^0 background is the mean of the impact parameters, κ_B, for those tracks. We used a value of 54.6 μm as determined from tracks kinematically similar to the D^0 candidates (Fig. 10(b)). We estimate the error of κ_B to be ± 15 μm which corresponds to ± 3 μm in $c\tau$. The overall error from the non-D^0 background is then ± 5 μm.

2) Bottom Contribution (δ, κ_b)

The contribution from b-quarks depends on the ratio $\Gamma(b \to c \to D)/\Gamma(b \to c \to D^*)$. In the Monte Carlo, this was set to unity. When the ratio is varied between 4 to 1/4, the resulting $c\tau$ changes at most ± 3 μm. The value of the average b-hadron lifetime, κ_b, also affects the result. We change the average b-lifetime between 0.7 and 2.3×10^{-12} sec[17,18] to get corresponding $c\tau$ errors of $^{+6}_{-7}$ μm. Since the above two systematics are not correlated, they are added in quadrature to give $^{+7}_{-8}$ μm.

3) Mass Assignments

The mass assignment affects the lifetime through the multiple scattering error $\sigma_{\text{m.s.}}$. The leading tracks are selected by the Čerenkov counter and the effect of the misidentification is negligible. Also, the non-leading tracks in the K-mode can be safely assumed to be pions. However, the non-leading 'K' tracks in the

π-mode are not all kaons. Even if we assume them to be all pions the resulting $c\tau$ increases by only 3 μm.

4) Track Momentum Cut

Removing the cut changes the result by less than 1 μm. Setting the cut at 750 MeV/c instead of 250 MeV/c removes 49 tracks, giving a lifetime of 134^{+51}_{-58} μm. Thus, there is no indication of bias from the track momentum cut.

5) Impact Parameter Window

Our fit is relatively insensitive to the window because of the inclusion of the flat tail in the likelihood function. Changing the cut value in the range $\pm$0.5mm around the standard value of 2.5 mm, the variation in $c\tau$ is found to be $^{+7}_{-4}$ μm.

6) Expected Impact Parameter Error (σ)

There are several factors that contribute to the expected error in the impact parameter as shown in (3.2). However, they are highly correlated in the sense that the result has to fit the impact parameter distribution in the final data. The χ^2 of the expected impact parameter distribution to the binned data increase at least one unit when the σ's are scaled by 0.9 and 1.1, which in turn translates to the error in $c\tau$ of $^{+14}_{-7}$ μm. The smaller the σ the larger the lifetime.

7) $\eta \sin\theta$ Cut

This cut removes the tracks that have little significance in the fit. Removing the cut brings in 173 tracks and the lifetime becomes 126 ± 45 μm. No significant improvement in the error is observed. We take the systematic error due to this cut to be $^{+0}_{-10}$ μm.

8) Errors In η And $\sin\theta$

The direction and the momentum of the D^0 are well determined. When

a track is taken correctly, the probability of mistaking the sign of the impact parameter due to the error in the D^0 direction is found to be much less than 1% in the Monte Carlo, and the effect can be safely ignored. Also, the resolutions of η and $\sin\theta$ are found to have negligible effect on the result.

The above items are expected to be independent of each other, and thus they are added quadratically. The items that have to be treated linearly have been already done so inside each category. The final overall systematic error in $c\tau$ is $^{+18}_{-16}$ μm.

5. Summary And Discussion

We have measured the lifetime of D^0 meson using impact parameters of D^0 tracks with respect to the beam center given by a beam position monitor. The maximum likelihood method used has been found to be bias free. Also, we have found the impact parameter method to be insensitive to various effects such as nuclear interactions at the beam pipe, small misalignments of drift chambers, etc. The measured $c\tau$ is 136^{+46+18}_{-46-16} μm which corresponds to the lifetime of $4.6^{+1.5+0.6}_{-1.5-0.5} \times 10^{-13}$sec. This is consistent with the world average[7] $3.9 \pm 0.4 \times 10^{-13}$sec.

It is expected that the semileptonic decay rate of D^0 is the same as that of $D^{\pm}$, which is based on the assumption that the semileptonic decays of the two mesons do not depend on the flavor of the spectator quark. This assumption can be checked by comparing the ratio of the lifetimes with the ratio of the semileptonic branching fractions. If the semileptonic decay rate is the same for the two mesons, the two ratios should be equal. Using the world average of the $D^{\pm}$ lifetime[7] $8.2^{+1.1}_{-0.9} \times 10^{-13}$sec, we obtain $\tau_{D^+}/\tau_{D^0} = 1.8 \pm 0.7$ which is consistent

with the recent measurement[2] $\mathrm{Br}(D^+ \to eX)/\mathrm{Br}(D^0 \to eX) = 2.3^{+0.5+0.1}_{-0.4-0.1}$, thus supporting the assumption.

The standard theory can predict the D^0 semileptonic decay rate as a function of the effective charm quark mass,[4]

$$\Gamma_{\mathrm{sl}} = \Gamma_\mu \left(\frac{M_c}{M_\mu}\right)^5 g\gamma_{\mathrm{QCD}}$$

where Γ_μ is the muon decay rate, M_c is the effective charm quark mass, M_μ is the muon mass, g is the phase space factor, and γ_{QCD} is the QCD correction factor. Small variations in M_c result in large changes in Γ_{sl}. Thus, a measurement of the semileptonic decay rate can determine the effective quark mass precisely. This value is a measure of the phase space available to the decay, and expected to be larger than the current quark mass which is estimated to be around 1.2 GeV/c^2.[22] However, the effective quark mass is expected to lie between the meson mass and the current quark mass. Our D^0 lifetime, together with the D^0 semileptonic branching fraction[2] of $7.5 \pm 1.1 \pm 0.4\%$, gives a D^0 semileptonic decay rate Γ_{sl} of $1.6 \pm 0.6 \times 10^{11}\mathrm{sec}^{-1}$. For $g = 0.56 \pm 0.11$ and $\gamma_{\mathrm{QCD}} = 0.85 \pm 0.05$,[23] the effective charm quark mass in a D^0 meson is $M_c = 1.58 \pm 0.12$ GeV/c^2, which is in the range of typical constituent charm quark mass but substantially larger than the current charm quark mass.

ACKNOWLEDGEMENTS

We wish to thank M.Peskin for stimulating discussions. We also acknowledge the contributions to DELCO by the technical staffs of Caltech, SLAC Group A, SLAC Group G, and the PEP Division. A.C. and G.B. thank the French National Scientific Research Center, and E.E. the A. v. Humboldt Foundation.

(a) Present address: CERN, CH-1211, Geneva 23, Switzerland.

(b) Present address: Watkins-Johnson Co., 2525 North First Street, San Jose, CA 95131-1097.

(c) Present address: U. of Victoria, Dept. of Physics, P.O. Box 1700, Victoria, B.C. V8W 2Y2, Canada.

(d) Present address: DESY, F-22, Notkestrasse 85, D-2000 Hamburg 52, West Germany.

(e) Present address: Department of Physics, Beijing University, Beijing, The People's Republic of China.

(f) Present address: Institute of High Energy Physics, P.O. Box 918, Beijing, The People's Republic of China.

(g) Present address: National Lab. for High Energy Physics, KEK, Oho-machi, Tsukuba-gun, Ibaraki-ken, 305 Japan.

(h) Present address: Spectra Physics, 3333 North 1st St, San Jose, Ca. 95134-1995.

(j) Present address: L.A.P.P., Annecy-Le-Vieux, BP 909 France 74019.

(i) Present address: Fakultät für Physik, Albert-Ludwigs-Universität, Hermann -Herder Strasse 3, 7800 Freiburg, West Germany.

(k) Present address: Ford Aerospace, 3939 Fabian Way, Mail Stop G-82, Palo Alto, CA. 94303.

(l) Present address: University of Geneva, Dept. of Physics, 32 Boulevard d'Yuoy, 1211 Geneva, Switzerland.

(m) Present address: Hughes Aircraft Co., Mail Station R8-2660, P.O. Box 92426, L.A. Ca. 90009.

(n) Present address: NYCB Realtime Computing Inc., 106 Rocky Point Gardens, Rock Point, NY 11778.

REFERENCES

1. W.Bacino *et al.*, Phys. Rev. Lett. **45**, 329 (1980); R.H.Schindler *et al.*, Phys. Rev. D**24**, 78 (1981);
2. R.M.Baltrusaitis *et al.*, SLAC Reort No. SLAC-PUB-3532 (to be published).
3. Among others, a mechanism to enhance the D^0 non-leptonic decay rate is the W-exchange model: M.Bander, D.Silverman, and A.Soni, Phys. Rev. Lett. **44**, 7 (1980); H.Fritzsch and P.Minkowski, Phys. Lett. **90B**, 455 (1980). And a mechanisms to suppress the $D^{\pm}$ non-leptonic decays is the final state interference in $D^{\pm}$ decay: B.Guberina, S.Nussinov, R.Peccei, and R.Ruckl, Phys. Lett. **89B**, 111 (1979). Also, see the references in: L-L.Chau, Phys. Rep. **95**, 1 (1983).
4. N.Cabibbo and L.Maiani, Phys. Lett. **79B**, 109 (1978).
5. G.Altarelli *et al.*, Nucl. Phys. **B208**, 365 (1982), and the references therein.
6. The semileptonic decay rate of charged D's may be larger than that of neutral D's by up to $\approx 10\%$ if the annihilation channel, which is Cabbibo suppressed, is important. U.Baur and H.Fritzsch, Phys. Lett. **109B**, 402 (1982).
7. See, for example: N.W.Reay, Proceedings of the International Symposium on Lepton and Photon Interactions at High Energies, Ithaca, 1983.
8. J.M.Yelton *et al.*, Phys. Rev. Lett. **52**, 2019 (1984).
9. For a general description of the DELCO detector, see: Particle Data Group, Lawrence Berkeley Laboratory Report No. LBL-91 Suppl. UC-37 (1983).

10. The expected horizontal beam sizes are obtained from $\sigma_x^2 = \beta_x^* \epsilon_{x0}/2$, where β_x^* is the value of the horizontal beta function at interaction regions and ϵ_{x0} is the emittance, both calculated from the configuration of the storage ring.

11. Particle Data Group, Rev. Mod. Phys. **56** No.2, (1984), pS50.

12. The effect of tracks from heavy quarks is found to be negligible in estimating $\sigma_{\rm trk}$.

13. S.Nussinov, Phys. Rev. Lett., **35**, 1672 (1975).

14. H.Yamamoto *et al.*, Phys. Rev. Lett. **54**, 522 (1985).

15. The Monte Carlo uses the LUND e^+e^- event generator (T.Sjöstrand, Comp. Phys. Commun. **28**, 229 (1983)) and includes detailed simulations of drift chamber hits and Čerenkov responses. The $c\tau$'s used in the Monte Carlo are; 420 μm for hadrons containing a b-quark, 130 μm for D^0, 280 μm for D^+, 60 μm for F^+, and 70 μm for Λ_c. For the strange particles, the values are taken from: Particle Data Group, Rev. Mod. Phys. **56** No.2, (1984). The effect of the strange particles on the width of gaussian is small.

16. An upper limit on $\Gamma(b \to ul\nu)\ /\Gamma(b \to cl\nu)$ of 4% has been set by A.Chen *et al.*, Phys. Rev. Lett. **52**, 1084 (1984).

17. N.Lockyer *et al.*, Phys. Rev. Lett. **51**,1316 (1983); E.Fernandez *et al.*, Phys. Rev. Lett. **51**,1022 (1983); M.Althoff *et al.*, Phys. Lett. **149b**,524 (1984);

18. D.Klem *et al.*, Phys. Rev. Lett. **53**,1873 (1984);

19. That the formula (4.1) satisfies the consistency requirement can be shown as

follows. Assume for notational simplicity that all events have an identical window and configuration, and let l^0 be the true $c\tau$. The probability distribution of b is then $f^0(b,l^0)db$. For the case when the number of tracks N tends to infinity, the most likely l is given by

$$\begin{aligned}\frac{\partial \mathcal{L}}{\partial l} &= -2\sum_{i=1}^{N}\frac{\partial f(b^i,l)}{\partial l}f(b^i,l)^{-1} \\ &= -2\int_{b_1}^{b_2}\frac{\partial f(b,l)}{\partial l}f(b,l)^{-1} \times \text{const.} \times f^0(b,l^0)db \\ &= 0\end{aligned}$$

The true value l^0 should be a solution of this equation. Substituting l^0 for l everywhere in the last equation, we get,

$$\frac{\partial}{\partial l^0}\int_{b_1}^{b_2} f(b,l^0)db = 0$$

In other words, the integration of the probability function $f(b,l)$ in (b_1,b_2) cannot be a function of l, and this requirement is clearly satisfied by (4.1).

20. The large round-off error that occurs when κ is small can be avoided by using an approximation $xe^{x^2}\text{erfc}(x) = 0.564190 - 0.274030/x^2$ for x^2 greater than $\approx$50. For example see: M.Abramowitz and I.Stegun, Handbook of Mathematical Functions, p316, (National Bureau of Standards 1972).
21. Some bins with small number of counts have been combined.
22. For example see: J.Gasser and H.Leutwyler, Phys. Rep. **87**, 77 (1982).
23. The value and error of g correspond to $M_s/M_c = 0.28 \pm 0.05$. The QCD correction factor γ_{QCD} depends on the value of $\Lambda_{\overline{\text{MS}}}$, which is taken to be 150 ± 100 MeV. (See for example Ref. 4).

TABLE CAPTIONS

1. Beam sizes obtained by Bhabha tracks and the expected values from the machine parameters.
2. The means of the impact parameter for the D^0 sample and the three control samples.
3. The fraction of the tracks from D^0 decays in each track category. The definition of the correction factor $r_{\rm corr}$ is in the text.

Table 1

(μm)		82	83	84
measured	σ_x	462 ± 6	369 ± 6	342 ± 4
	σ_y	113 ± 10	75 ± 17	83 ± 12
expected	σ_x	380	420	420
	σ_y	$\lesssim 100$	$\lesssim 100$	$\lesssim 100$

Table 2

$< b >$ (μm)	data	MC
D^0 candidates	151.7±42.3	—
(a) general tracks	40.7±1.5	34.9±1.6
(b) selected tracks	54.6±12.0	43.4±11.7
(c) general tracks*	1.1±1.5	1.0±1.2

* thrust axis randomized

Table 3

		r_{corr}	Purity
K-mode	K	1.09	$0.94 \pm 0.03 \pm 0.02$
	π	0.93	$0.80 \pm 0.03 \pm 0.04$
π-mode	K	1.16	$0.67 \pm 0.07 \pm 0.07$
	π	1.48	$0.85 \pm 0.09 \pm 0.05$

FIGURE CAPTIONS

1. The definition of the impact parameter and its sign. All parameters are defined in the plane perpendicular to the beam axis. The point O is the beam center given by the beam position monitor. The impact parameter b is defined as $|\vec{b}|$ with the sign of $\vec{b} \cdot \vec{P}_{\perp D^0}$. The cases for a positive and negative b are shown in (a) and (b) respectively.

2. The side view of the DELCO detector.

3. The x coordinate of the interaction points of Bhabha events, in the detector frame (a), and relative to the beam position given by the monitor (b). The horizontal axis is the event time in an arbitrary unit. The same set of figures for the y coordinate is given in (c) and (d).

4. The beam variance vs ϕ. The measurement error is already subtracted. The solid curve is the results of the fits to the shape $\sigma_x^2 \cos^2\phi + \sigma_y^2 \sin^2\phi$.

5. The error due to the tracking $\sigma_{\rm trk}$ is plotted against the error given by the track fitting program, $\sigma_{\rm fit}$. The solid curve is a function fitted to the data points. The broken lines are the root-mean-squares of $\sigma_{\rm m.s.}$ and $\sigma_{\rm beam}$ in each bin.

6. The impact parameter distribution is plotted for each bin of the overall expected error, σ. In each plot the center value of σ is indicated in unit of cm, and the curve is the result of fit with the expected gaussian plus a flat background.

7. The mass difference $\Delta M = M_{K\pi\pi_{D^*}} - M_{K\pi}$ for the K-mode (a), and for the π-mode (b). The distributions for wrong sign candidates (shaded) are plotted over those for right sign candidates. The arrows show the position

of ΔM cut.

8. The $\eta \sin\theta$ distribution for each type of track in the D^0 sample (data).
9. The impact parameter distributions for the D^0 candidate tracks in the D^* sample.
10. The impact parameter distributions for: (a) the general tracks in hadronic events, (b) the tracks kinematically similar to the D^0 tracks, and (c) the same as the first but with the thrust axis randomized.
11. The fraction of tracks that comes from b-particle decays as a function of the D^0 momentum.
12. The shape of $f^0(b, \kappa, \sigma)$ is shown for $\sigma = 500$ μm (fixed) and κ =100 (a), 400 (b), and 700 μm (c).
13. One sigma contour of the likelihood fit. The two parameters are the level of the tail γ and the D^0 lifetime $c\tau$.
14. (a) The simulated $\mathcal{L}_{\rm min}$ using the measured $c\tau$ of 136 μm and the actual event configuration of each event in the data. The arrow indicates the $\mathcal{L}_{\rm min}$ for the actual data. The distribution of $c\tau$ obtained at the same time is shown in (b).

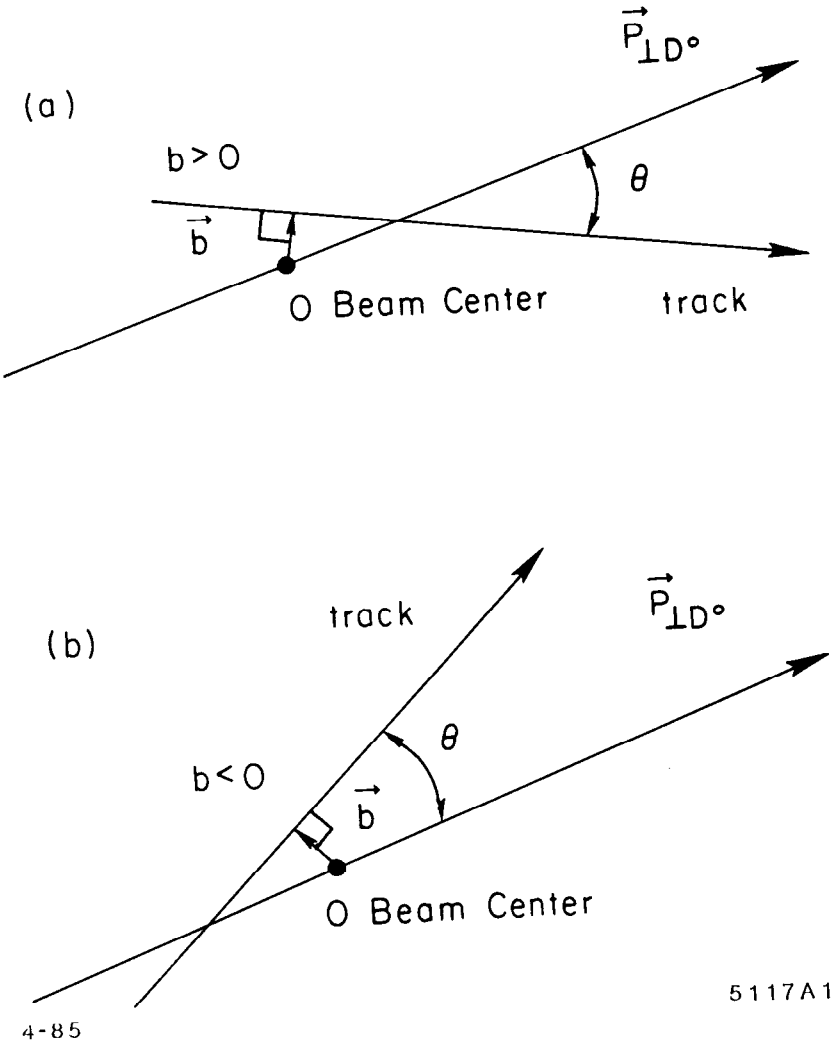
(a)
$\vec{P}_{\perp D^0}$
b>0
θ
$\vec{b}$
O Beam Center
track
(b)
track
$\vec{P}_{\perp D^0}$
θ
b<0
$\vec{b}$
O Beam Center
5117A1
4-85

Fig. 1

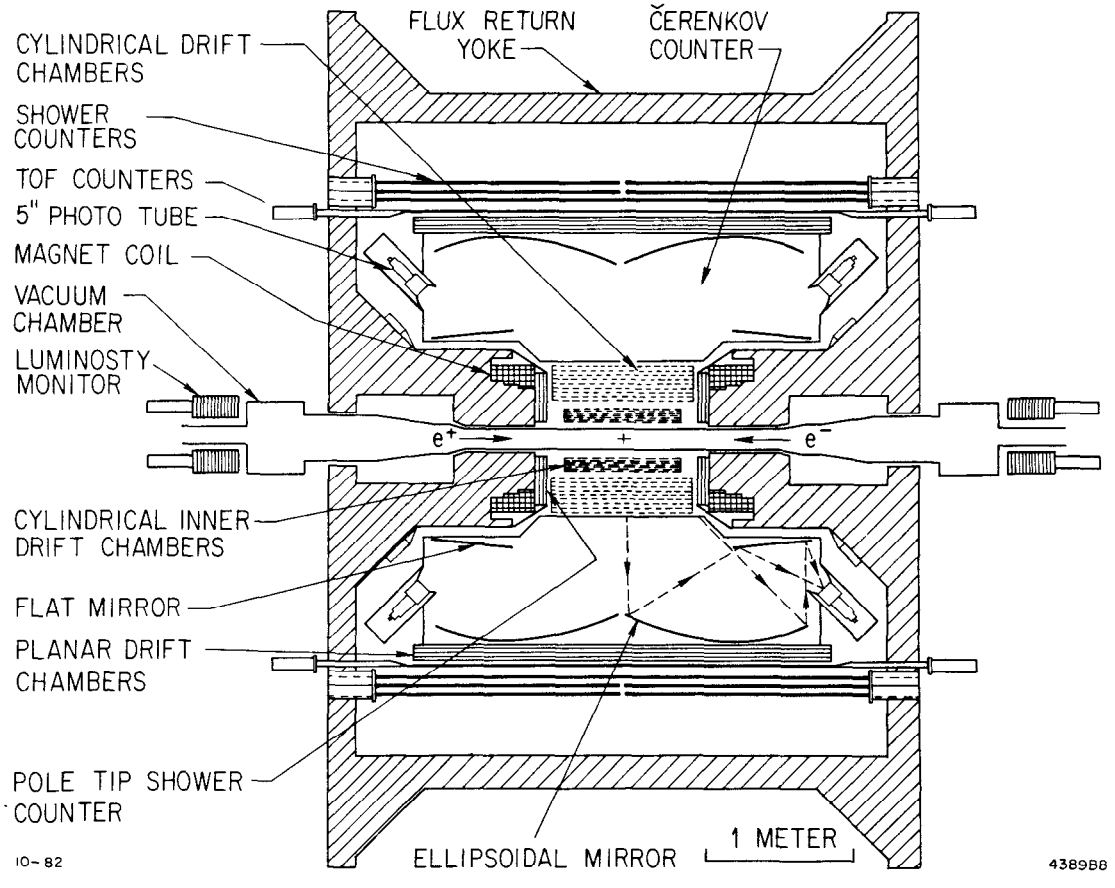
CYLINDRICAL DRIFT CHAMBERS
SHOWER COUNTERS
TOF COUNTERS
5" PHOTO TUBE
MAGNET COIL
VACUUM CHAMBER
LUMINOSTY MONITOR
CYLINDRICAL INNER DRIFT CHAMBERS
FLAT MIRROR
PLANAR DRIFT CHAMBERS
POLE TIP SHOWER COUNTER
FLUX RETURN YOKE
ČERENKOV COUNTER
e+
e−
ELLIPSOIDAL MIRROR
1 METER
10-82
4389B8

Fig. 2

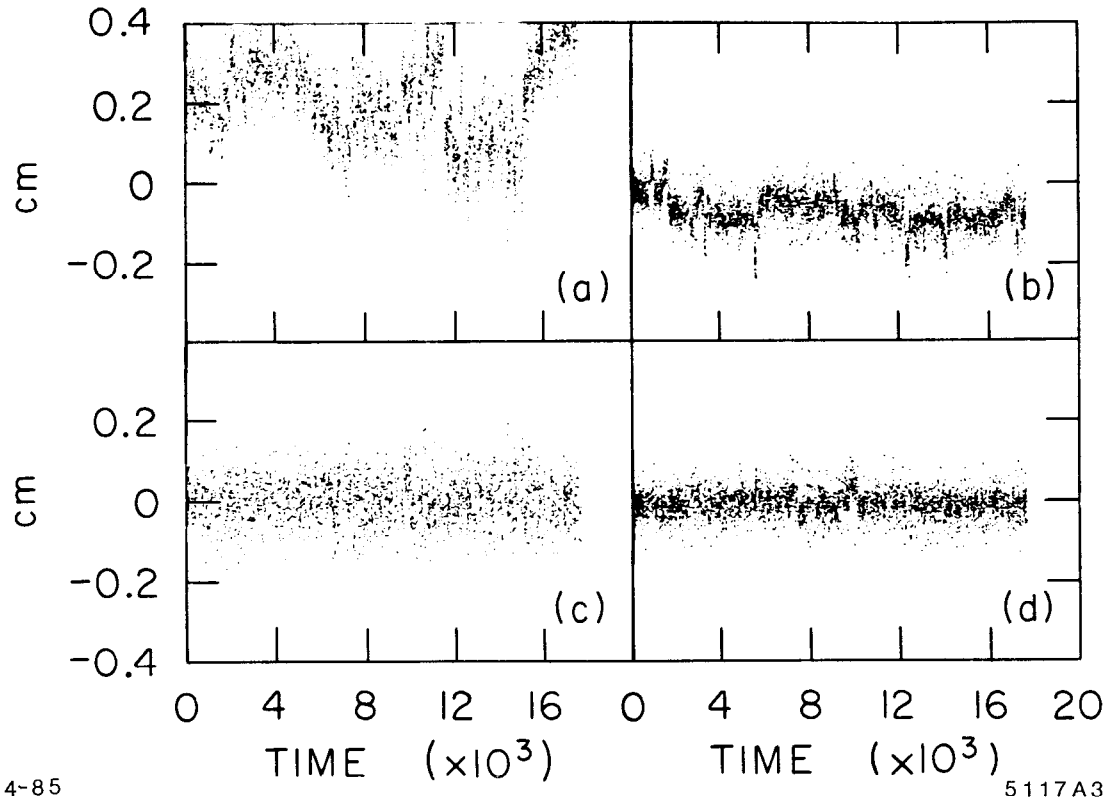
0.4
0.2
0
-0.2
cm
(a)
(b)
0.2
0
-0.2
-0.4
cm
(c)
(d)
0 4 8 12 16
0 4 8 12 16 20
TIME (×10³)
TIME (×10³)
4-85
5117A3

Fig. 3

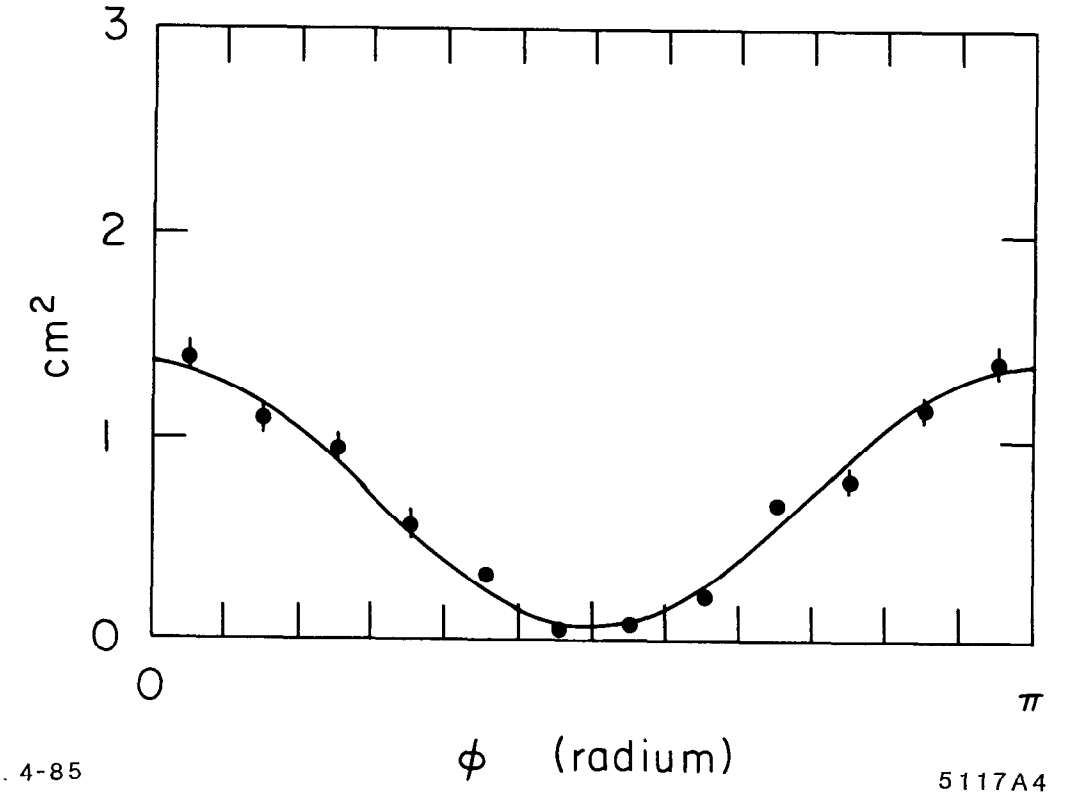

Fig. 4

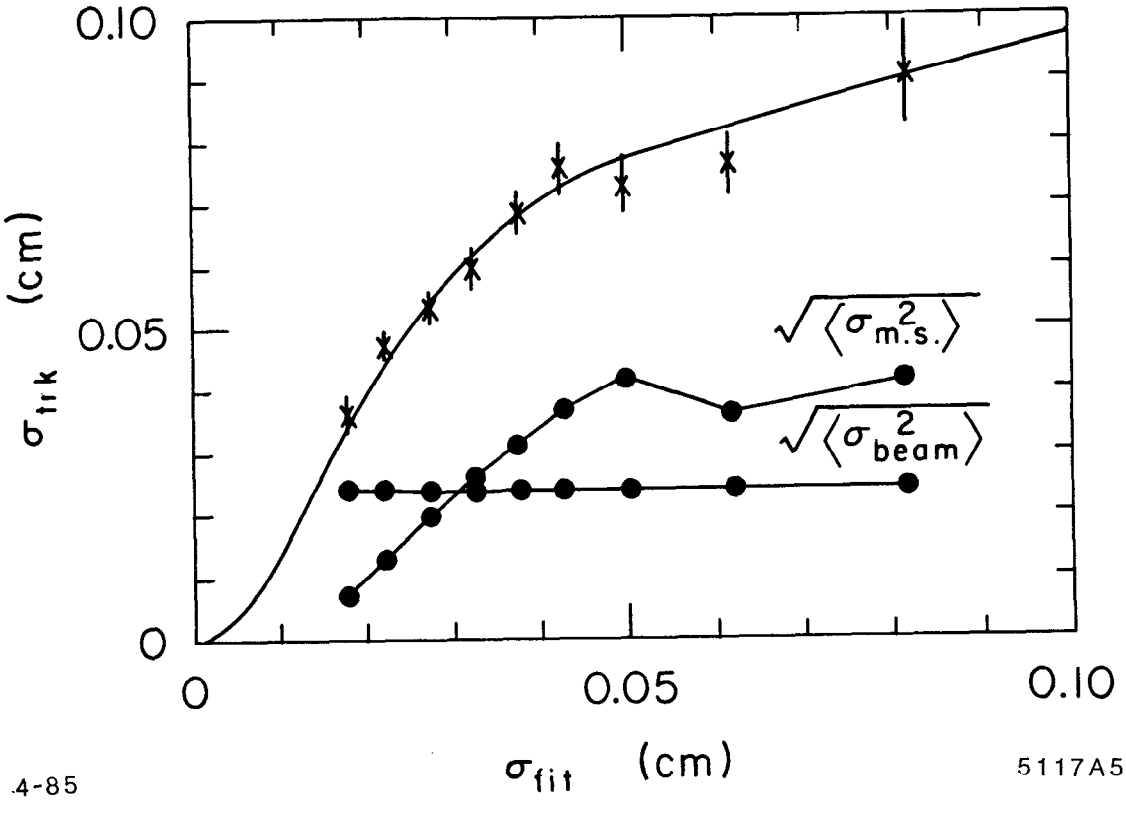
0.10
0.05
0
σ_{trk} (cm)
$\sqrt{\langle \sigma^2_{m.s.} \rangle}$
$\sqrt{\langle \sigma^2_{beam} \rangle}$
0
0.05
0.10
σ_{fit} (cm)
4-85
5117A5

Fig. 5

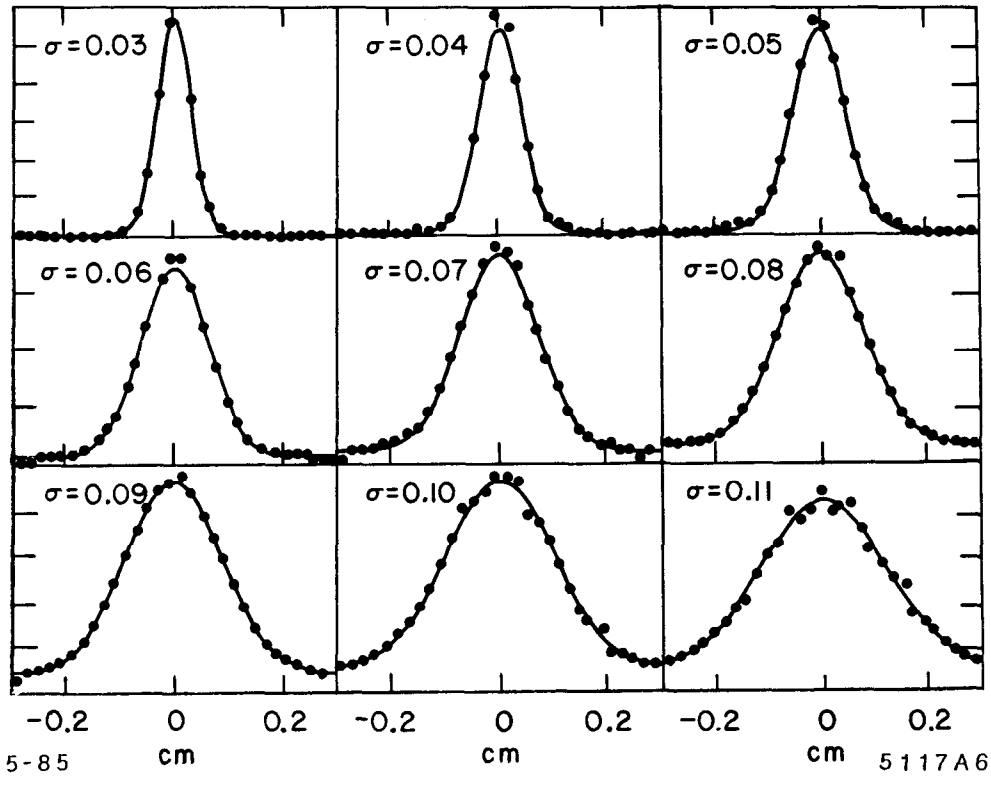
σ=0.03
σ=0.04
σ=0.05
σ=0.06
σ=0.07
σ=0.08
σ=0.09
σ=0.10
σ=0.11
-0.2
0
0.2
cm
5-85
5117A6

Fig. 6

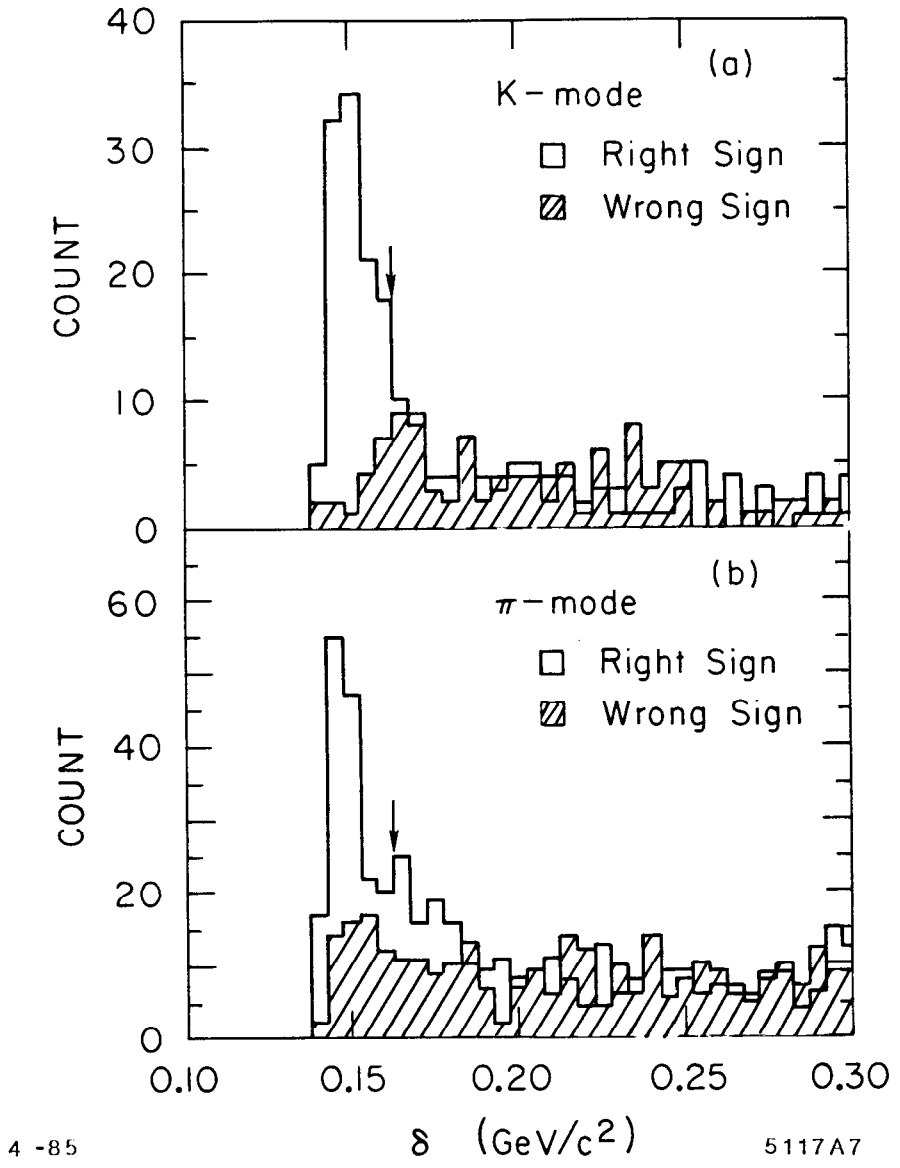
40
30
20
10
0
COUNT
(a)
K − mode
Right Sign
Wrong Sign
60
40
20
0
COUNT
(b)
π − mode
Right Sign
Wrong Sign
0.10
0.15
0.20
0.25
0.30
δ (GeV/c²)
4 -85
5117A7

Fig. 7

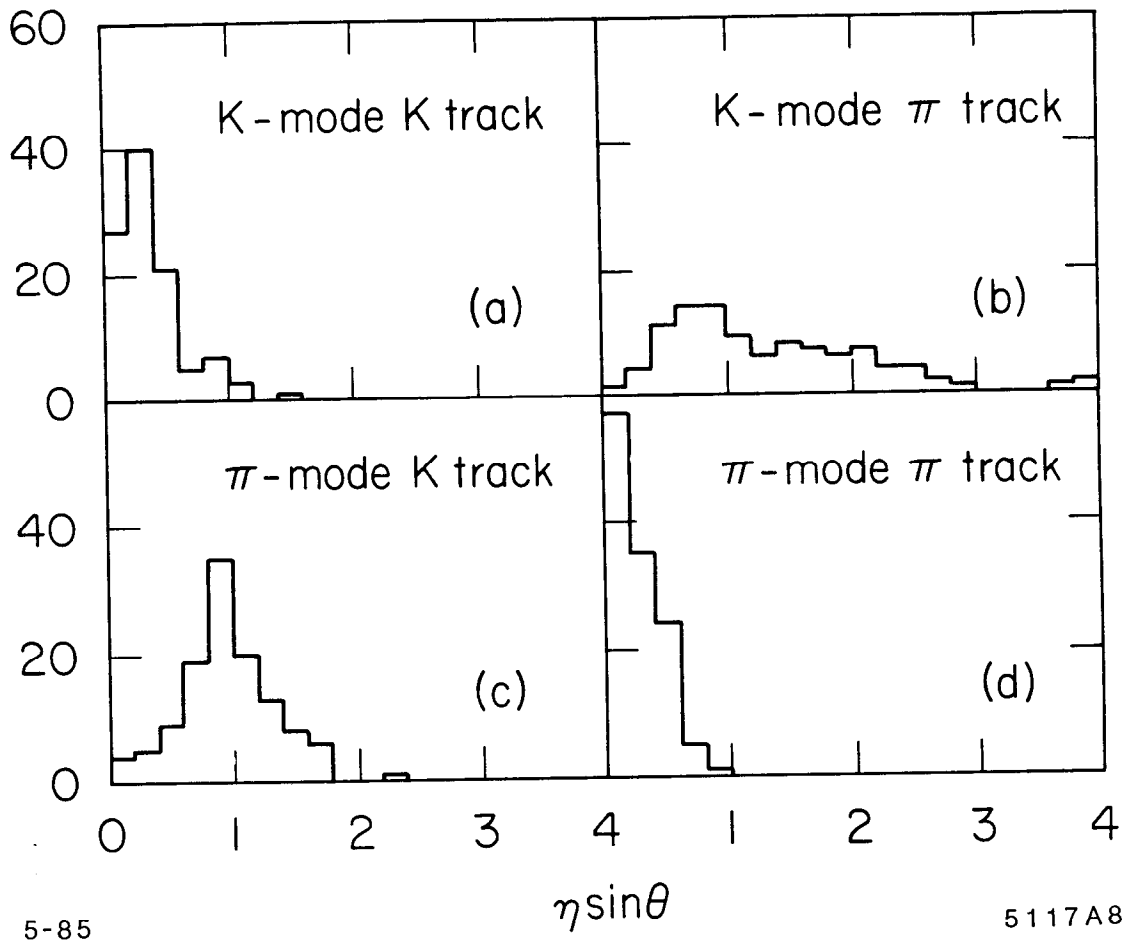
60
40
20
0
K - mode K track
(a)
K - mode π track
(b)
π - mode K track
(c)
π - mode π track
(d)
40
20
0
0
1
2
3
4
1
2
3
4
ηsinθ
5-85
5117A8

Fig. 8

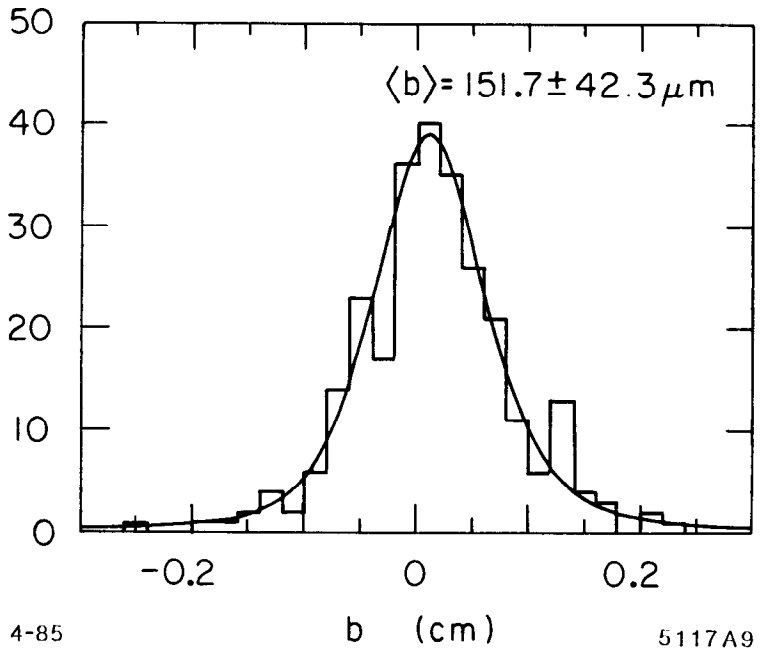

Fig. 9

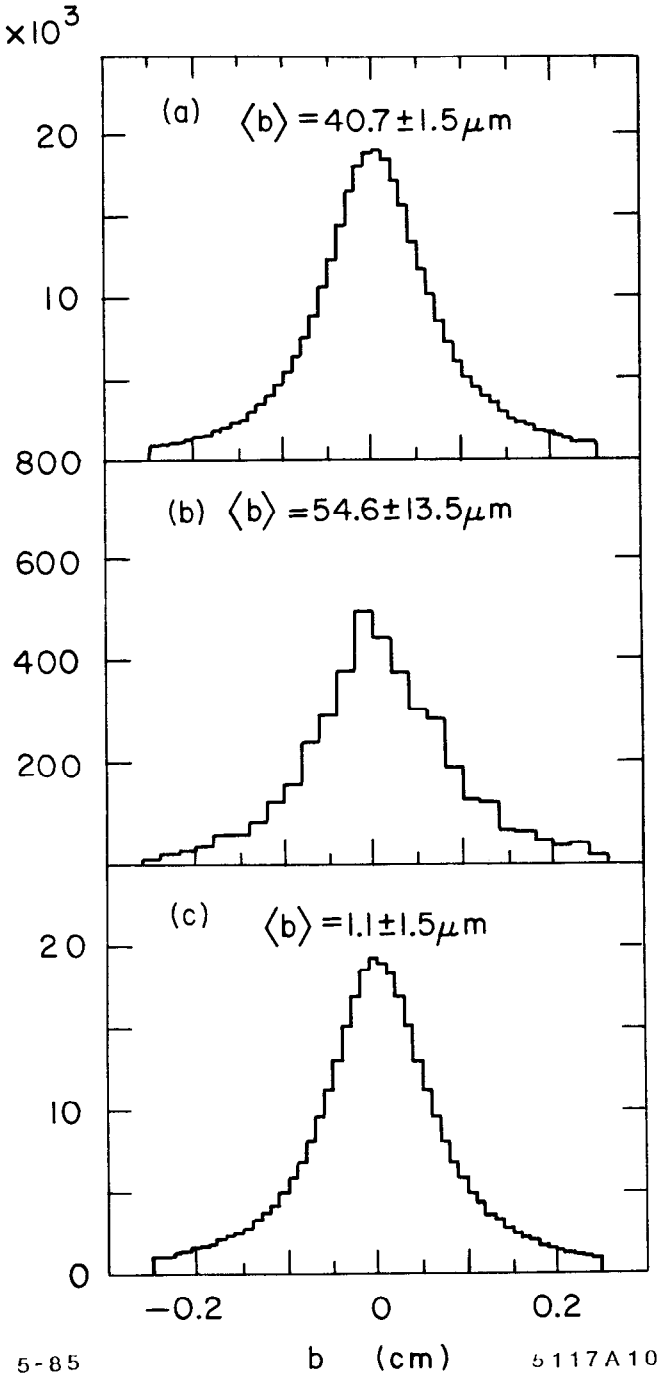
×10^3
(a) ⟨b⟩ = 40.7 ± 1.5 μm
(b) ⟨b⟩ = 54.6 ± 13.5 μm
(c) ⟨b⟩ = 1.1 ± 1.5 μm
20
10
800
600
400
200
20
10
0
−0.2
0
0.2
b (cm)
5-85
5117A10

Fig. 10

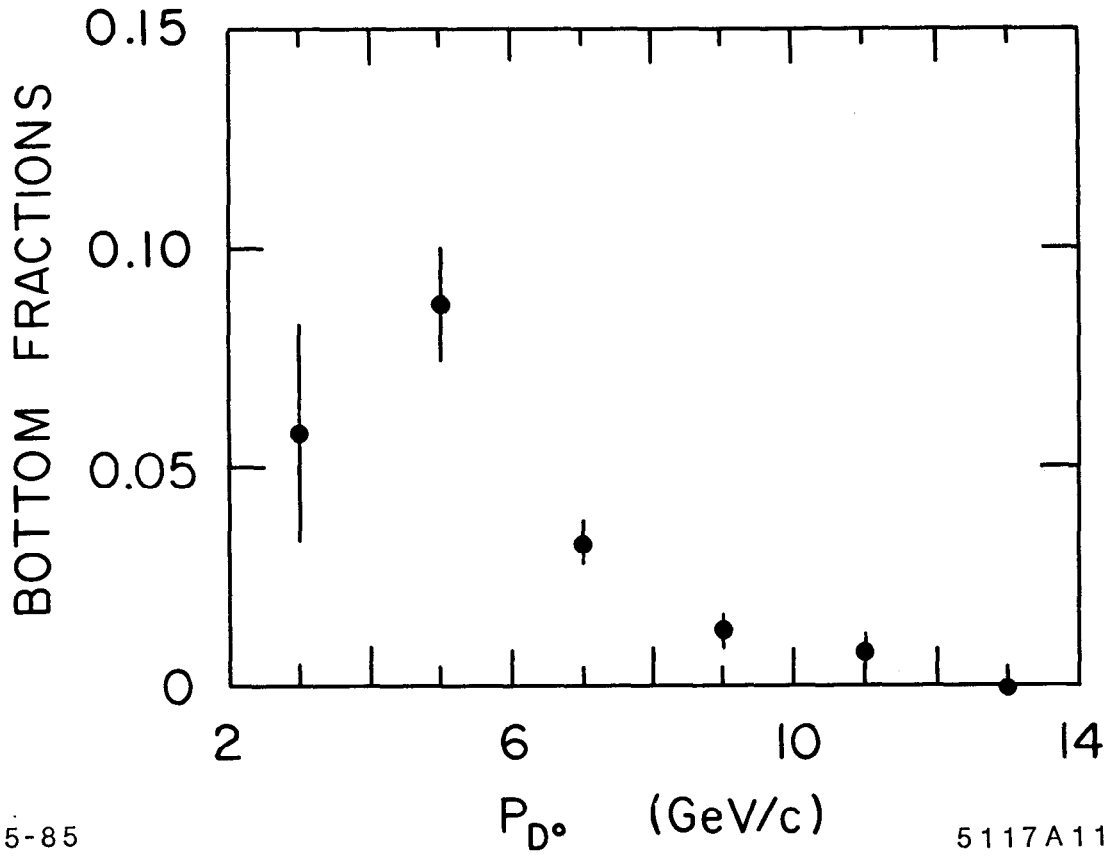

Fig. 11

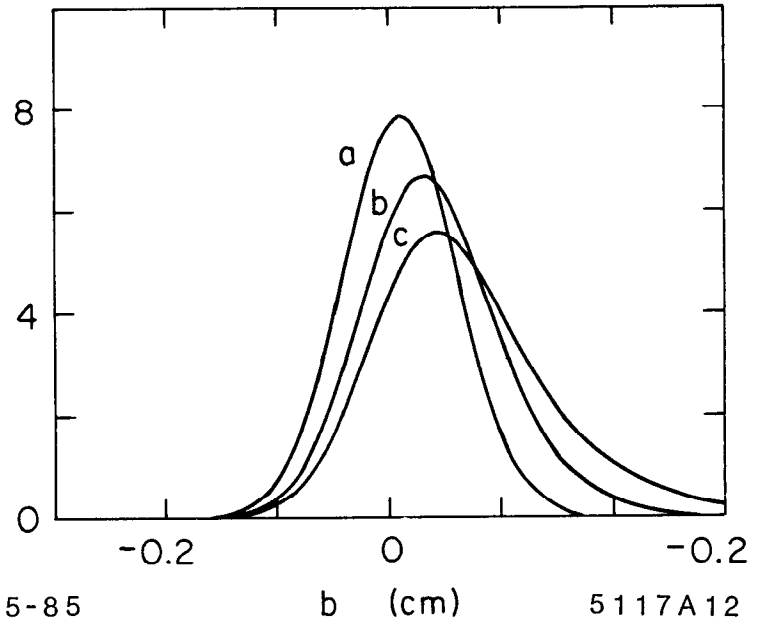

Fig. 12

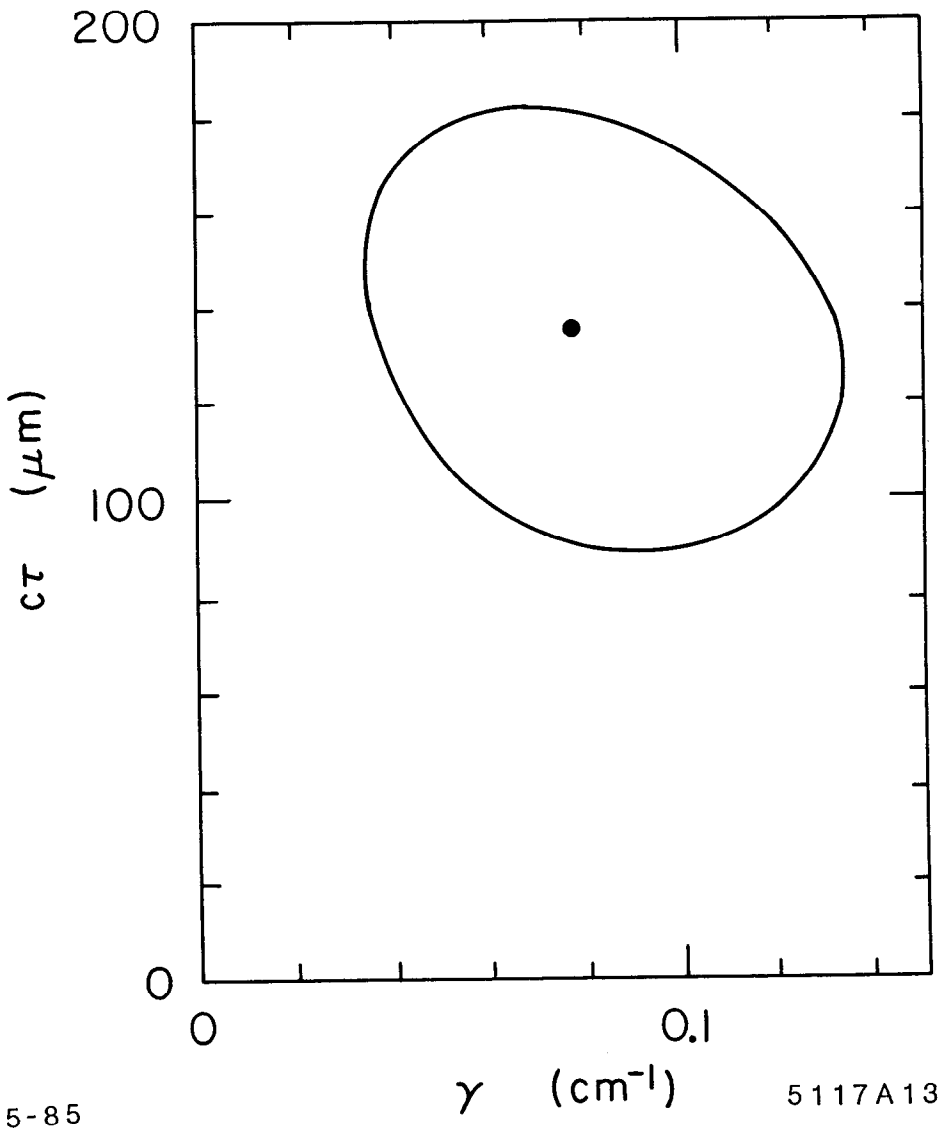

Fig. 13

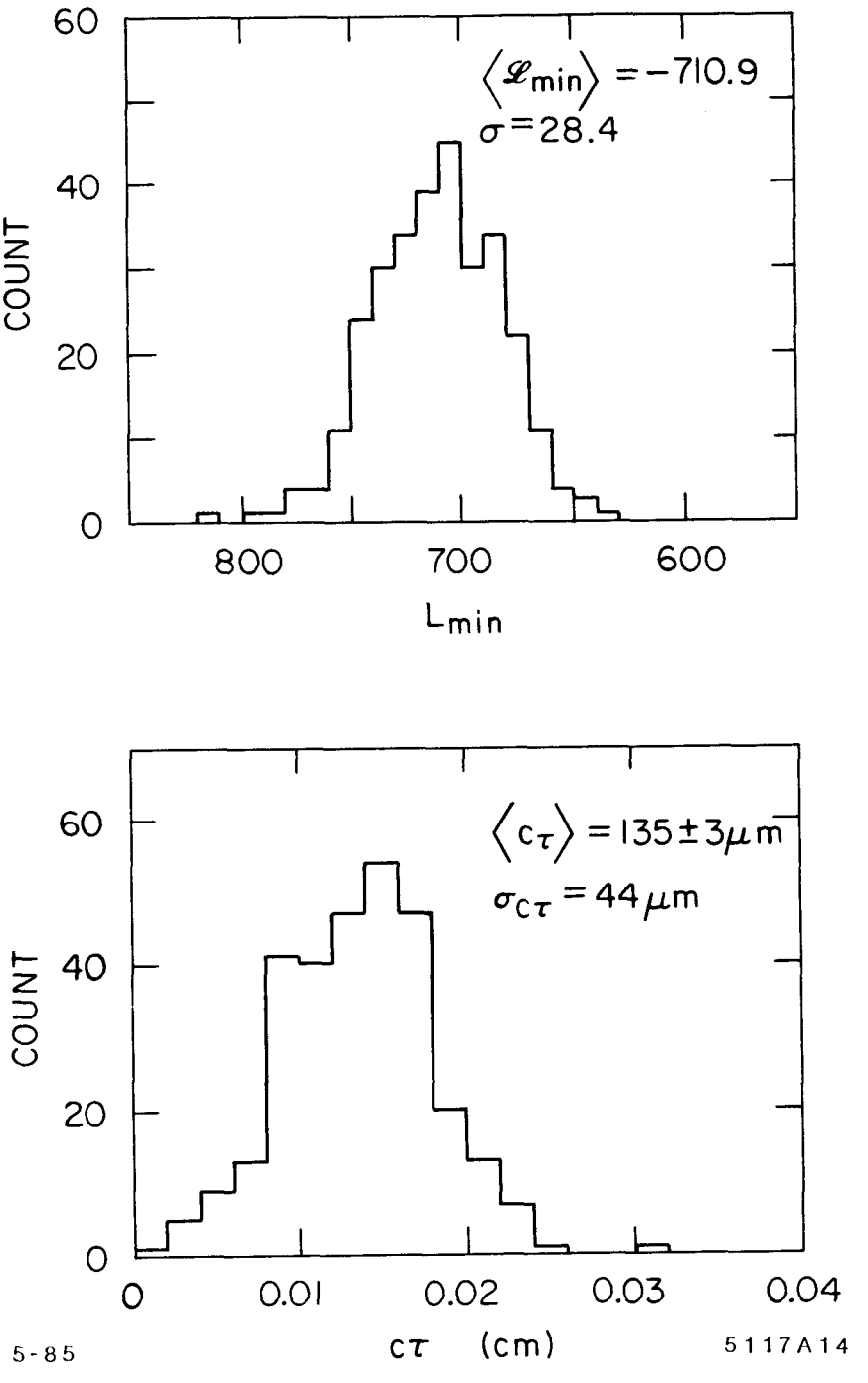
60
40
20
0
COUNT
$\langle \mathscr{L}_{min} \rangle = -710.9$
$\sigma = 28.4$
800
700
600
L_{min}
60
40
20
0
COUNT
$\langle c\tau \rangle = 135 \pm 3\mu m$
$\sigma_{c\tau} = 44\mu m$
0
0.01
0.02
0.03
0.04
$c\tau$ (cm)
5-85
5117A14

Fig. 14